Impaired frontal-parietal control network in chronic prostatitis/chronic pelvic pain syndrome (CP/CPPS) revealed by graph theoretical analysis: a DTI study

Xinfeng Huang
Department of Andrology, Jiangsu Province Hospital of Chinese Medicine, Affiliated Hospital of Nanjing University of Chinese Medicine, Nanjing, China

Jianhuai Chen (jianhuaichen@126.com)
Jiangsu Province Academy of Traditional Chinese Medicine

Jie Yang
Department of Urology, Jiangsu Provincial People's Hospital, First Affiliated Hospital of Nanjing Medical University, Nanjing, China

Shaoying Yuan
Department of Andrology, Zhuhai Hospital of the Traditional Chinese Medicine Hospital of Guangdong Province, Zhuhai, China

Zhan Qin
Department of Andrology, Zhuhai Hospital of the Traditional Chinese Medicine Hospital of Guangdong Province, Zhuhai, China

Hongliang Cui
Department of Urology, Nantong Hospital of Traditional Chinese Medicine, Nantong, China

Tao Liu
Department of Andrology, Jiangsu Province Hospital of Chinese Medicine, Affiliated Hospital of Nanjing University of Chinese Medicine, Nanjing, China

Yongkang Zhu
Department of General Surgery, Jiangsu Province Hospital of Chinese Medicine, Affiliated Hospital of Nanjing University of Chinese Medicine, Nanjing, China

Yun Chen
Department of Andrology, Jiangsu Province Hospital of Chinese Medicine, Affiliated Hospital of Nanjing University of Chinese Medicine, Nanjing, China

---

Research

Keywords: Chronic prostatitis/chronic pelvic pain syndrome, Diffusion tensor imaging, White matter, Graph theory, Small-world

Posted Date: March 4th, 2020

DOI: https://doi.org/10.21203/rs.3.rs-15934/v1

Version of Record: A version of this preprint was published at European Journal of Neuroscience on December 15th, 2020. See the published version at https://doi.org/10.1111/ejn.14962.

Abstract

Introduction Chronic prostatitis/chronic pelvic pain syndrome (CP/CPPS) is characterized by chronic pain in pelvic area and lower urinary tract symptoms (LUTS). Previous neuroimaging studies demonstrated that chronic pain was associated with altered brain activity. However, the pathological mechanisms associated with altered brain control of CP/CPPS is not well understood. Therefore, we sought to investigate the topological properties of white matter brain networks in patients with CP/CPPS and whether the topological configuration of frontal-parietal control network was disrupted.

Methods We collected 19 patients with CP/CPPS and 32 matched healthy controls (HCs). Diffusion tensor imaging data of all participates were used to map the white matter structural networks. Graph theoretical method was applied to investigate the alterations of topological properties of brain network in patients. Moreover, the associations between the alerted brain regions of patients and clinical measurements were analysised by using Pearson correlation analyses.

Results Both CP/CPPS patients and HCs exhibited a 'small-world' behaviour or economical small-world architecture of the white matter brain networks. In addition, CP/CPPS had a lower global efficiency in the right middle frontal gyrus (orbital part) and a higher global efficiency in the left middle cingulate and paracingulate gyri. CP/CPPS also showed decreased local efficiency in the left middle cingulate and paracingulate gyri and paracentral lobule. Moreover, the local efficiency of the left middle cingulate gyrus was positively correlated with the scores of the influence of symptoms on the quality of life. The local efficiency of the left precuneus and right supplementary motor area were positively correlated with the total scores of NIH-CPSI and the scores of pain and discomfort symptoms, respectively.

Conclusion Together, we found that patients with CP/CPPS had alterations of connections within the frontal-parietal control network, which suggested that the altered connectivity involved in the executive control processing procedures might contribute to the pathogenesis of the pelvic pain and LUTS in CP/CPPS. Thus these results providing new insights into the understanding of CP/CPPS.

1. Background

Prostatitis is a highly prevalent urologic condition, which is characterized by a wide range of pelvic pain or discomfort and lower urinary tract symptoms (LUTS)[1]. Chronic prostatitis/Chronic pelvic pain syndrome (CP/CPPS) is the most frequent form of prostatitis, which has a tremendous impacts on the quality of life[2]. CP/CPPS is defined as a heterogeneous condition associated with pelvic pain, voiding symptoms and/or sexual dysfunction, which last for at least 3 of the previous 6 months[3]. The diagnosis and monitoring of CP/CPPS is often based on the investigations, such as structured symptom assessment (the National Institutes of Health Chronic Prostatitis Symptom Index, NIH-CPSI)[3]. Moreover, the diagnosis of CP/CPPS can be made after ruling out obvious etiologic causes, such as active urethritis[4]. CP/CPPS is associated with a complex and heterogeneous etiology and its specific pathophysiology has been incompletely understood[5]. Therefore, no specific and validated biomarkers

for the diagnosis and severity assessment of CP/CPPS has been found so far. In addition, The heterogeneity has made finding effective treatment for CP/CPPS regimens challenging.

Recent evidence suggested that the etiologies of CP/CPPS included inflammatory or noninflammatory etiologies, such as autoimmune mechanisms, the peripheral sensitization caused by the inflammation factors and central neurologic mechanisms[6]. Additionally, CP/CPPS is also considered to be associated with the psychological function including negative emotional, cognitive and behavioral consequences, which have been found to influence the function and structure of the brain[7–9]. Therefore, both the peripheral inflammation or neurological damage and altered brain function can lead to impaired control function of pelvic floor neuromuscular and/or neuropathic pain[10–12]. The central nervous system has been proved to play a vital role in the pain modulation[13]. Distinct patterns of pain related brain activation have been found in both acute and chronic pain conditions[14]. Moreover, chronic pain often results from a combination of peripheral and central processes, which produces long-term changes in how and where pain is processed by the brain[15].

Control of the bladder and urethra also depends on the brain (supraspinal neuronal network), which provides the ability to voluntarily voiding[16]. The function of brain regions controlling the voiding reflex were found to be abnormal when bladder sensation becomes strong in patients with disorders of bladder control[17]. Previous neuroimaging study demonstrated that activity in frontal cortex, parietotemporal lobe, cingulate gyrus, insula, parahippocampus and cuneus were correlated with the urgency incontinence clinical severity[18, 19]. Functional magnetic resonance image (fMRI) study have also showed that the activity of higher order cognitive control brain regions are increased in normal subjects during bladder filling and voiding[20]. Therefore, exploring the the brain regions associated with the LUTS is key to identifying central abnormalities in patients with CP/CPPS.

Given previous evidence of abnormal function in CP/CPPS[8, 21], we predicted that CP/CPPS patients also had disrupted the topological organization in the brain structural networks. Therefore, we applied a graph-theoretical analysis to diffusion tensor imaging (DTI) data and compared the topological properties of the white matter brain networks between patients with CP/CPPS and healthy controls (HCs). In particular, we focused on the analysis of small-world efficiency of the brain networks and examined whether the altered brain regions were associated with the clinical variables of CP/CPPS.

2. Materials And Methods

2.1. Subjects

We recruited 19 right-handed patients with CP/CPPS, and 32 age, education matched right-handed HCs (Table 1). This study was approved by the ethical committee of the Affiliated Hospital of Nanjing University of Chinese Medicine. Additionally, written informed consents were obtained from all participats.

Table 1

Demographic and clinical characteristics of CP/CPPS and HC.

Variables	CP/CPPS (n = 32)	HC (n = 35)	t value	P value
Age (years)	38.11 ± 9.02	33.94 ± 8.53	1.65	0.11
Educational level (years)	14.05 ± 2.61	14.25 ± 1.92	-0.31	0.76
Total scores of NIH-CPSI	25.21 ± 6.80	-	-	-
Scores of pain and discomfort symptoms	9.89 ± 4.07	-	-	-
Scores of symptom severity	16.00 ± 5.11	-	-	-
Scores of urination symptom	6.11 ± 3.28	-	-	-
Scores of the influence of symptoms on the quality of life	9.21 ± 2.78	-	-	-
CP/CPPS: chronic prostatitis/chronic pelvic pain syndrome; HCs: health controls. $P < 0.05$ indicated significant between-groups differences.				

The inclusion criterias for patients with CP/CPPS were as follows: 1) 20–45 years old; 2) had complaints about the symptoms of pelvic discomfort/pain for 3 or more months within the last 6months; 3) the total scores of NIH-CPSI ≥ 15; 4) had negative prostate cultures. The exclusion criterias for all participats consisted of the following: 1) had any sexual dysfunction; 2) had a history of head trauma; 3) had any serious psychiatric and organic diseases including urological, neurological, cardiovascular, respiratory, gastrointestinal, endocrine diseases, etc; 4) had a history of using of alcohol or any drugs that had effects on the brain function or structure, such as psychotropic drugs; 5) had any contraindications to undergo MRI scan.

In addition, the scale of NIH-CPSI was selected to assess the lower urinary tract symptoms (LUTS) and pelvic pain or discomfort of all participates.The individual question scores, subdomain scores, and total scores of the NIH-CPSI questionnaire were obtained.

2.2. MRI Data Acquisition

The T1-weighted images and DTI data were obtained by using a 3.0 T Siemens Verio scanner. Anatomical images were performed with T1 weighted 3D sagittal acquisition (repetition time (TR), 1900 ms; echo time (TE), 2.48 ms; slice thickness, 1 mm; matrix size, 256 × 256; field of view (FOV), $250mm^2 \times 250mm^2$; flip angle (FA), 9°; slice thickness, 1 mm)[22]. The whole-brain diffusion MRI sequence using diffusion tensor spin echo planar imaging was acquired (TR, 6600 ms; TE, 93 ms, matrix size,128 ×

128; FOV, 240mm^2 × 240mm^2; thickness, 3 mm; number of slices, 45). In addition, DTI datas were acquired along 30 non-linear directions with gradient values b = 0 and 1000s/mm^2[23].

2.3. MRI Data Preprocessing

T1-weighted images and DTI data were processed by using the Functional MRI of the Brain (FMRIB) software Library (FSL) (FSL, http://www.fmrib.ox.ac.uk/fsl.html)[24]. Firstly, T1-weighted images were segmented and DTI data were corrected for eddy current distortions and head motion by applying an affine alignment of the diffusion-weighted images to the b0 images. Secondly, the diffusion tensor matrix of all participates were calculated by solving the Stejskal and Tanner equation. Thirdly, the fractional anisotropy (FA) of each voxel was calculated and FA maps of all participates were calculated. Finally, individual diffusion-weighted images of all participant were coregistered to their T1-weighted images and then were normalized to the Montreal Neurological Institute (MNI) space using a nonlinear transformation.

In addition, to reconstruct the whole-brain white matter (WM) tracts, DTI tractography was carried out using the diffusion toolkit (http://trackvis.org/dtk/) based on the Fiber Assignment by Continuous Tracking (FACT) algorithm. Then the fiber tracts between brain regions were estimated. The propagation of tractography was terminated if it turned an angle > 50° or reached a voxel with an FA < 0.2[25]. Finally, the streamlines of all participates were normalized to the MNI-152 space.

2.4. Network Construction

The nodes and edges are the two basic elements of the brain network. The procedures of defining the nodes and edges of the brain network have been previously described in previous neuroimaging studies[26–28].

2.4.1. Node Definition

In this study, the automated anatomical labeling (AAL) template was employed to segment the entire brain into 90 regions of interest (ROIs) (45 cortical and subcortical regions for each hemisphere), each representing a node of the brain network[29]. Therefore, the 90 ROIs were defined as the nodes of the brain network.

2.4.1. Edge Definition

The edges correspond to the structural connectivities between all possible pairs of brain regions. Two ROIs were considered structurally connected when the fibers connected with these two regions ≥ 2 and the length > 5mm[25]. The identified structural connections were defined as the edges between the nodes of the structural brain network. For the weighted brain network, we defined the the mean FA values of the connected fibers between two ROIs as the weights of the structural brain network.

2.5. Brain Network Analysis

2.5.1 Small-world efficiency

The small-world property of the network were originally proposed by Wattz and Strogatz (1998)[30]. However, previous studies demonstrated the global efficiency and local efficiency were more suitable parameters for characterizing the properties of small-world efficiency of the weighted networks[31, 32]. Therefore, we employed the network efficiency measures to quantify the small-world behaviour of the structural brain networks in CP/CPPS, which supported the efficient transfer of parallel information at relatively low cost of the brain network (economical small-world properties).

The global efficiency (E_glo_net) and local efficiency (E_loc_net) of the brain network were calculated using the brain connectivity toolbox, as well as the global efficiency (E_glo_rand) and local efficiency (E_loc_rand) of the matched random networks[33]. More detailed interpretations of the method could be found in previous studies[31, 33]. The brain network was considered to have the small-world behaviour if it met the following criterias: $E\_glo\_normal = E\_glo\_net/E\_glo\_rand \approx 1$ and $E\_loc\_normal = E\_loc\_net/E\_loc\_rand > 1$, Where E_glo_normal and E_loc_normal were the normalized global and local efficiency values of the brain networks[28].

2.5.2 Network and regional nodal efficiency

Two measures for the nodal (regional) characteristics of structural networks were quantified: the nodal local efficiency and global efficiency.

The nodal global efficiency was computed as the inverse of the mean harmonic shortest path length between this brain region and all other regions in the brain network. The nodal local efficiency was the global efficiency of the subgraph of the neighbors of this brain region. More detailed about the calculation of these two parameters had been described in previous studies[31, 33].

The nodal global efficiency could quantify the importance of the brain region for communication within the brain network, which indicated the level of its role for the hub region. The nodal local efficiency could measure the fault tolerance of the brain region, which indicated how well the information was communicated between the neighbors of a brain region when that region was removed.

2.6. Statistical Analysis

Statistical analysis was performed using SPSS 20 software (Chicago, IL, USA). To determine the significant differences of the brain network properties between groups, an analysis of two-sample t-test was conducted (The threshold value for establishing significance was set at $P < 0.05$). To correct for multiple comparisons, P was subjected to a false-discovery rate (FDR) threshold of $q = 0.05$. In addition, the correlations between the network properties and the clinical variables (the scores of NIH-CPSI) of CP/CPPS patients were assessed using the Pearson correlation (The statistical significance threshold of was set at $P < 0.05$ (uncorrected)).

3. Results

3.1. Small-world efficiency of the WM brain networks in CP/CPPS

Graph theoretical analysis revealed that the WM brain networks of both CP/CPPS and HCs had a much higher local efficiency (CP/CPPS: t = 15.63,P = 0.00; HCs: t = 31.84, P = 0.00) and a similar global efficiency (CP/CPPS: t=-1.69,P = 0.10; HCs: t= -1.49, P = 0.14) compared with those of the matched random networks (Table 2; Fig. 1A). In other words, compared with HCs, the CP/CPPS WM brain networks also exhibited a 'small-world' behaviour or economical 'small-world' properties, which was indicative high topological efficiency (Table 2; Fig. 1A). Therefore, the WM brain networks demonstrated efficient small-world architecture and had an economical behaviour for both CP/CPPS and HCs, which supported the efficient transfer of parallel information of the brain networks at relatively low cost. In addition, there were no statistically significant differences between the two groups in the values of small-world efficiency (t=-0.23, P = 0.82) (Table 2; Fig. 1B).

Table 2
Small-world efficiency of WM brain networks and between-group differences.

		CP/CPPS	HCs	t	P
Global efficiency	E_glo_net	0.13 ± 0.028	0.13 ± 0.013	-0.32	0.75
	E_glo_ rand	0.14 ± 0.031	0.14 ± 0.014	-0.15	0.88
	E_glo_ normal	0.89 ± 0.023	0.89 ± 0.020	-1.14	0.26
Local efficiency	E_loc_net	0.23 ± 0.047	0.22 ± 0.028	0.81	0.42
	E_loc_rand	0.054 ± 0.013	0.050 ± 0.0099	1.34	0.19
	E_loc_ normal	4.45 ± 1.30	4.57 ± 0.94	0.42	0.71
Small-world efficiency		5.03 ± 1.52	5.12 ± 1.10	-0.23	0.82

CP/CPPS: chronic prostatitis/chronic pelvic pain syndrome; HCs: health controls; WM: white matter; E_glo_net: the global efficiency of the brain network; E_glo_rand: the global efficiency of the matched random networks; E_glo_normal: the normalized global efficiency of the brain network; E_loc_net: the local efficiency of the brain network; E_loc_rand: the local efficiency of the matched random networks; E_loc_normal: the normalized local efficiency of the brain network. P < 0.05 indicated significant between-groups differences.

3.2. Network efficiency of the whole brain in CP/CPPS

The small-world efficiency parameters included the network local efficiency and network global efficiency, as well as the normalized network local efficiency and normalized network global efficiency. However, compared with HCs, the CP/CPPS patients exhibited no significant differences in the values of the

network local (t = 0.81, P = 0.42) and global efficiency (t=-0.32, P = 0.75) (Table 2; Fig. 1C). Moreover, there were also no significant differences of the normalized network local (t = 0.42, P = 0.71)and global efficiency (t=-1.14, P = 0.26) between CP/CPPS and HCs (Table 2; Fig. 1D).

3.3. Regional nodal efficiency of the brain networks in CP/CPPS

To determine the regional nodal characteristics of the WM structural networks in the CP/CPPS patients, we computed two measures of efficiency: the nodal local efficiency and global efficiency.

Compared with HCs, patients with CP/CPPS had a lower global efficiency in the right middle frontal gyrus (orbital part) (survived FDR-correction) and a higher global efficiency in the left middle cingulate and paracingulate gyri (survived FDR-correction) (Table 3; Fig. 2A). However, the between-group differences (uncorrected $P < 0.05$) of the left supplementary motor area, postcentral gyrus and paracentral lobule did not survive FDR-correction (Table 3; Fig. 2A).

Table 3

Brain regions with abnormal nodal global and local efficiency in patients with CP/CPPS.

Brain regions		CP/CPPS	HCs	t	P
Global efficiency					
Frontal	ORBmid.R	0.095 ± 0.046	0.13 ± 0.015	-3.71	0.00052
	SMA.L	0.12 ± 0.023	0.11 ± 0.014	2.07	0.044
	DCG.L	0.16 ± 0.027	0.14 ± 0.019	3.52	0.00096
Parietal	PoCG.L	0.14 ± 0.022	0.12 ± 0.018	2.88	0.0059
	PCL.L	0.13 ± 0.019	0.11 ± 0.015	2.71	0.0092
Local efficiency					
Frontal	PreCG.L	0.27 ± 0.047	0.22 ± 0.049	2.92	0.0053
	ORBmid.R	0.19 ± 0.10	0.25 ± 0.050	-2.84	0.0066
	SMA.L	0.24 ± 0.093	0.19 ± 0.061	2.33	0.024
	SMA.R	0.21 ± 0.11	0.15 ± 0.074	2.36	0.022
	DCG.L	0.25 ± 0.075	0.19 ± 0.036	3.76	0.00045
	DCG.R	0.21 ± 0.071	0.17 ± 0.052	2.70	0.0095
Parietal	PCG.L	0.32 ± 0.10	0.27 ± 0.079	2.11	0.040
	PoCG.L	0.26 ± 0.053	0.22 ± 0.045	2.82	0.0069
	SPG.L	0.27 ± 0.057	0.23 ± 0.057	2.51	0.015
	SMG.R	0.25 ± 0.026	0.23 ± 0.035	2.076	0.043
	PCUN.L	0.26 ± 0.073	0.22 ± 0.049	2.30	0.025
	PCL.L	0.25 ± 0.088	0.17 ± 0.065	3.83	0.00036
Temporal	PHG.R	0.19 ± 0.076	0.15 ± 0.056	2.019	0.049
	STG.R	0.24 ± 0.029	0.21 ± 0.033	2.66	0.011

CP/CPPS: chronic prostatitis/chronic pelvic pain syndrome; HCs: health controls; L: left; R: right; ORBmid: middle frontal gyrus (orbital part); SMA: supplementary motor area; DCG: middle cingulate and paracingulate gyri; PoCG: postcentral gyrus; PCL: paracentral lobule; PreCG: precental gyrus; SMA: supplementary motor area; PCG: posterior cingulate gyrus; PHG: parahippocampal gyrus; SPG: superior parietal gyrus; SMG: supramarginal gyrus; PCUN: precuneus; STG: superior temporal gyrus. $P < 0.05$ indicated significant between-groups differences. Bold font indicated the between-group differences survived FDR-correction.

Morover, CP/CPPS patients showed decreased local efficiency in the left middle cingulate and paracingulate gyri (survived FDR-correction) and paracentral lobule (survived FDR-correction) (Table 3; Fig. 2B). The differences of local efficiency (uncorrected $P < 0.05$) in the left precental gyrus, supplementary motor area, posterior cingulate gyrus, postcentral gyrus, superior parietal gyrus and precuneus, right middle frontal gyrus (orbital part), supplementary motor area, middle cingulate and paracingulate gyri, supramarginal gyrus, parahippocampal gyrus and superior temporal gyrus did not survive FDR-correction (Table 3; Fig. 2B).

3.4. Relationships between altered nodal efficiency and NIH-CPSI

In the patient group, the local efficiency of the left middle cingulate gyrus (survived FDR-correction) was positively correlated with the scores of the influence of symptoms on the quality of life ($r = 0.60$; $P = 0.0065$) (Fig. 3A). In addition, the local efficiency of the left precuneus (not survived FDR-correction) ($r = 0.46$; $P = 0.045$) and right supplementary motor area (not survived FDR-correction) ($r = 0.47$; $P = 0.043$) were positively correlated with the total scores of NIH-CPSI and the scores of pain and discomfort symptoms, respectively (Fig. 3B&C).

4. Discussion

In the present study, our results showed that the white matter brain networks of CP/CPPS patients had economical small-world architecture. In addition, disrupted regional topological organization, including nodal local and global efficiency of the brain network were found in patients with CP/CPPS, predominantly in the frontal-parietal control network. Moreover, the abnormal local efficiency of frontal-parietal network were associated with the scores of NIH-CPSI of CP/CPPS patients. These findings provide new insights into the understanding of the structural architecture of the white matter brain networks in patients with CP/CPPS.

Previous neuroimaging studies demonstrated that human brain had a small-world architecture, which was capable of efficiently transferring information at a low wiring cost[34, 35]. Moreover, human brain has two organizational principles (functional segregation and integration), which support the balance between local specialization and global integration of brain structural and functional connectivity[36, 37]. Therefore, the abnormal small-world efficiency might lead to the impaired segregated and integrated information processing of the brain network, which are associated with the failure of functional integration within the brain[31].

However, we found that the overall small-world network efficiency (network efficiency metric) in CP/CPPS was not disrupted, while regional efficiency (nodal efficiency metric) was impaired in specific brain regions of the frontal-parietal control network. The results of economical small-world architecture demonstrated that the brain structural networks of CP/CPPS patients had high global and local efficiency of parallel information processing at a low wiring cost. The results of nodal efficiency suggested that the

brain of CP/CPPS was not optimally organized to support distributed and modularized information processing within the frontal-parietal control network. Therefore, our findings suggested that the brain of CP/CPPS patients had the principle of parallel information processing at a low cost, which was compatible with previous neuroimaging studies. However, the optimal balance between local specialization and global integration within the frontal-parietal control network was impaired.

Although the white matter brain networks of CP/CPPS retained a small-world topology, the nodal global and local efficiency were impaired within the frontal-parietal control network. The global efficiency of the structural brain network is predominantly associated with long range white matter connections, which ensurs rapid interactions of information between remote brain regions involved in the cognitive processes[38, 39]. Lower global efficiency was found in the right middle frontal gyrus (orbital part) of CP/CPPS in our study, which suggested fewer long range connections were connected with the right middle frontal gyrus (orbital part). The frontal gyrus are involved in the process of executive control and the pain processing in human brain[40, 41]. Previous evidence demonstrated that pain catastrophizing had an influence on symptom severity of CP/CPPS patients[42, 43]. Previous studies showed that higher pain catastrophizing was associated with the abnormal structure of the the prefrontal cortex of CP/CPPS patients[21, 44]. Therefore, the white matter lesions within the long range connections might be associated with the the pelvic pain or discomfort of CP/CPPS.

In addition, CP/CPPS had a higher global efficiency in the left middle cingulate and paracingulate gyri. The middle cingulate is involved in different aspects of pain processing of patients with chronic pain, especially pain-related memory processes and involved in the cortical mechanism of pain sensitization[45, 46]. In addition, the middle cingulate is also associated with the sensory processing of pain, particularly with pain intensity[46]. Therefore, the increased global efficiency of left middle cingulate might lead to the higher level of chronic pain in CP/CPPS patients.

Moreover, CP/CPPS patients had decreased local efficiency in the left middle cingulate and paracingulate gyri and paracentral lobule. The local efficiency is predominantly associated with short range white matter connections between neighboring brain regions, which mediates modularized information processing between nearby brain regions[31]. Therefore, brain regions with aberrant local efficiency are considered to be vulnerable to adjacent white matter lesions and decreased local efficiency also reflects disrupted topological organizations of the brain networks in patients with CP/CPPS. Our results about the impaired local efficiency within the frontal-parietal control network suggested that CP/CPPS patients also had white matter lesions within the short range connections, which might be involved in the pain modulation process.

Finally, the impaired local efficiency of middle cingulate gyrus was associated with the reduced quality of life in CP/CPPS patients. The aberrant local efficiency within frontal-parietal control network was also related to the disease severity and pain symptoms. The catastrophizing and behavioural pain coping strategies are considered to be predictors for chronic pain in pelvic area and quality of life of CP/CPPS

patients. Therefore, these results provided evidence that anatomical brain abnormalities were related to the clinical features of CP/CPPS.

5. Conclusion

In this study, our results demonstrated that the brain structural networks of CP/CPPS exhibited economical small-world properties, which was characterized by a high local and global efficiency at a relatively low wiring cost. However, disrupted nodal local and global efficiency were found in the frontal-parietal control network of patients with CP/CPPS.The impaired nodal efficiency reflected white matter lesions within the short and long range connections and disrupted structural organization of spatially distributed brain regions. These findings further elucidated changes occurring in the structural architecture of the brain in patients with CP/CPPS.

Declarations

Competing interests

The authors declare that they have no competing financial interests.

Funding

This study was supported by by the grants of: Jiangsu Province Six Talent Peaks Project (No. 2015-WSN-050); “333” Project of Jiangsu Province (No. LGY2016016); National Natural Science Foundation of China (No. 81701433; 81871154); Nanjing Medical Technology Development Project (No. YKK17098).

Authors' contributions

Xinfei Huang, Yongkang Zhu and Yun Chen designed the experiments. Jianhuai Chen, Jie Yang, Zhan Qin, Hongliang Cui and Tao Liu contributed to clinical data collection and assessment. Jianhuai Chen and Shaoying Yuan analyzed the results. Xinfei Huang, Jianhuai Chen and Jie Yang wrote the manuscript. Xinfei Huang, Jianhuai Chen, Jie Yang, Yongkang Zhu and Yun Chen approved the final manuscript. All authors assisted with carrying out the experiments.

Acknowledgments

This study was supported by by the grants of: Jiangsu Province Six Talent Peaks Project (No. 2015-WSN-050); “333” Project of Jiangsu Province (No. LGY2016016); National Natural Science Foundation of China (No. 81701433; 81871154); Nanjing Medical Technology Development Project (No. YKK17098).

References

[1] Khan FU, Ihsan AU, Khan HU, Jana R, Wazir J, Khongorzul P, Waqar M, Zhou X. Comprehensive overview of prostatitis[J]. Biomed Pharmacother, 2017, 94(1064-1076.

[2] Magistro G, Wagenlehner FM, Grabe M, Weidner W, Stief CG, Nickel JC. Contemporary Management of Chronic Prostatitis/Chronic Pelvic Pain Syndrome[J]. Eur Urol, 2016, 69(2): 286-297.

[3] Anderson RU, Wise D, Nathanson BH. Chronic Prostatitis and/or Chronic Pelvic Pain as a Psychoneuromuscular Disorder-A Meta-analysis[J]. Urology, 2018, 120(23-29.

[4] Nickel JC, Shoskes DA, Wagenlehner FM. Management of chronic prostatitis/chronic pelvic pain syndrome (CP/CPPS): the studies, the evidence, and the impact[J]. World J Urol, 2013, 31(4): 747-753.

[5] Magri V, Wagenlehner F, Perletti G, Schneider S, Marras E, Naber KG, Weidner W. Use of the UPOINT chronic prostatitis/chronic pelvic pain syndrome classification in European patient cohorts: sexual function domain improves correlations[J]. J Urol, 2010, 184(6): 2339-2345.

[6] Parker J, Buga S, Sarria JE, Spiess PE. Advancements in the management of urologic chronic pelvic pain: what is new and what do we know?[J]. Curr Urol Rep, 2010, 11(4): 286-291.

[7] Kwon JK, Chang IH. Pain, catastrophizing, and depression in chronic prostatitis/chronic pelvic pain syndrome[J]. Int Neurourol J, 2013, 17(2): 48-58.

[8] Kutch JJ, Yani MS, Asavasopon S, Kirages DJ, Rana M, Cosand L, Labus JS, Kilpatrick LA, Ashe-Mcnalley C, Farmer MA, Johnson KA, Ness TJ, Deutsch G, Harris RE, Apkarian AV, Clauw DJ, Mackey SC, Mullins C, Mayer EA. Altered resting state neuromotor connectivity in men with chronic prostatitis/chronic pelvic pain syndrome: A MAPP: Research Network Neuroimaging Study[J]. Neuroimage Clin, 2015, 8(493-502.

[9] Huang L, Kutch JJ, Ellingson BM, Martucci KT, Harris RE, Clauw DJ, Mackey S, Mayer EA, Schaeffer AJ, Apkarian AV, Farmer MA. Brain white matter changes associated with urological chronic pelvic pain syndrome: multisite neuroimaging from a MAPP case-control study[J]. Pain, 2016, 157(12): 2782-2791.

[10] Breser ML, Salazar FC, Rivero VE, Motrich RD. Immunological Mechanisms Underlying Chronic Pelvic Pain and Prostate Inflammation in Chronic Pelvic Pain Syndrome[J]. Front Immunol, 2017, 8(898.

[11] Hu C, Yang H, Zhao Y, Chen X, Dong Y, Li L, Dong Y, Cui J, Zhu T, Zheng P, Lin CS, Dai J. The role of inflammatory cytokines and ERK1/2 signaling in chronic prostatitis/chronic pelvic pain syndrome with related mental health disorders[J]. Sci Rep, 2016, 6(28608.

[12] Farmer MA, Chanda ML, Parks EL, Baliki MN, Apkarian AV, Schaeffer AJ. Brain functional and anatomical changes in chronic prostatitis/chronic pelvic pain syndrome[J]. J Urol, 2011, 186(1): 117-124.

[13] Henry DE, Chiodo AE, Yang W. Central nervous system reorganization in a variety of chronic pain states: a review[J]. PM R, 2011, 3(12): 1116-1125.

[14] Alshelh Z, Marciszewski KK, Akhter R, Di Pietro F, Mills EP, Vickers ER, Peck CC, Murray GM, Henderson LA. Disruption of default mode network dynamics in acute and chronic pain states[J]. Neuroimage Clin, 2018, 17(222-231.

[15] Mitsi V, Zachariou V. Modulation of pain, nociception, and analgesia by the brain reward center[J]. Neuroscience, 2016, 338(81-92.

[16] Zuo L, Zhou Y, Wang S, Wang B, Gu H, Chen J. Abnormal Brain Functional Connectivity Strength in the Overactive Bladder Syndrome: A Resting-State fMRI Study[J]. Urology, 2019, 131(64-70.

[17] Khavari R, Boone TB. Functional brain imaging in voiding dysfunction[J]. Curr Bladder Dysfunct Rep, 2019, 14(1): 24-30.

[18] Tadic SD, Griffiths D, Schaefer W, Cheng CI, Resnick NM. Brain activity measured by functional magnetic resonance imaging is related to patient reported urgency urinary incontinence severity[J]. J Urol, 2010, 183(1): 221-228.

[19] Ketai LH, Komesu YM, Dodd AB, Rogers RG, Ling JM, Mayer AR. Urgency urinary incontinence and the interoceptive network: a functional magnetic resonance imaging study[J]. Am J Obstet Gynecol, 2016, 215(4): 449 e441-449 e417.

[20] Griffiths D, Tadic SD. Bladder control, urgency, and urge incontinence: evidence from functional brain imaging[J]. Neurourol Urodyn, 2008, 27(6): 466-474.

[21] Lin Y, Bai Y, Liu P, Yang X, Qin W, Gu J, Ding D, Tian J, Wang M. Alterations in regional homogeneity of resting-state cerebral activity in patients with chronic prostatitis/chronic pelvic pain syndrome[J]. PLoS One, 2017, 12(9): e0184896.

[22] Chen J, Yang J, Huang X, Lu C, Liu S, Dai Y, Yao Z, Chen Y, Yu M. Variation in Brain Subcortical Network Topology Between Men With and Without PE: A Diffusion Tensor Imaging Study[J]. J Sex Med, 2020, 17(1): 48-59.

[23] Chen J, Chen Y, Gao Q, Chen G, Dai Y, Yao Z, Lu Q. Impaired Prefrontal-Amygdala Pathway, Self-Reported Emotion, and Erection in Psychogenic Erectile Dysfunction Patients With Normal Nocturnal Erection[J]. Front Hum Neurosci, 2018, 12(157.

[24] Smith SM, Jenkinson M, Woolrich MW, Beckmann CF, Behrens TE, Johansen-Berg H, Bannister PR, De Luca M, Drobnjak I, Flitney DE, Niazy RK, Saunders J, Vickers J, Zhang Y, De Stefano N, Brady JM, Matthews PM. Advances in functional and structural MR image analysis and implementation as FSL[J]. Neuroimage, 2004, 23 Suppl 1(S208-219.

[25] Chen J, Chen Y, Gao Q, Chen G, Dai Y, Yao Z, Lu Q. Brain structural network topological alterations of the left prefrontal and limbic cortex in psychogenic erectile dysfunction[J]. Int J Neurosci, 2018, 128(5): 393-403.

[26] Chen J, Yang J, Huang X, Ni L, Fan Q, Liu T, Yao Z, Chen Y. Reduced segregation and integration of structural brain network associated with sympathetic and dorsal penile nerve activity in anejaculation patients: a graph-based connectome study[J]. Andrology, 2019,

[27] Chen J, Huang X, Lu C, Liu T, Dai Y, Yao Z, Chen Y. Graph analysis of DTI-based connectome: decreased local efficiency of subcortical regions in PE patients with high sympathetic activity[J]. Andrology, 2019,

[28] Chen JH, Yao ZJ, Qin JL, Yan R, Hua LL, Lu Q. Aberrant Global and Regional Topological Organization of the Fractional Anisotropy-weighted Brain Structural Networks in Major Depressive Disorder[J]. Chin Med J (Engl), 2016, 129(6): 679-689.

[29] Tzourio-Mazoyer N, Landeau B, Papathanassiou D, Crivello F, Etard O, Delcroix N, Mazoyer B, Joliot M. Automated anatomical labeling of activations in SPM using a macroscopic anatomical parcellation of the MNI MRI single-subject brain[J]. Neuroimage, 2002, 15(1): 273-289.

[30] Watts DJ, Strogatz SH. Collective dynamics of 'small-world' networks[J]. Nature, 1998, 393(6684): 440-442.

[31] He Y, Dagher A, Chen Z, Charil A, Zijdenbos A, Worsley K, Evans A. Impaired small-world efficiency in structural cortical networks in multiple sclerosis associated with white matter lesion load[J]. Brain, 2009, 132(Pt 12): 3366-3379.

[32] Yan H, Tian L, Wang Q, Zhao Q, Yue W, Yan J, Liu B, Zhang D. Compromised small-world efficiency of structural brain networks in schizophrenic patients and their unaffected parents[J]. Neurosci Bull, 2015, 31(3): 275-287.

[33] Rubinov M, Sporns O. Complex network measures of brain connectivity: uses and interpretations[J]. Neuroimage, 2010, 52(3): 1059-1069.

[34] Liao X, Vasilakos AV, He Y. Small-world human brain networks: Perspectives and challenges[J]. Neurosci Biobehav Rev, 2017, 77(286-300.

[35] Bullmore E, Sporns O. The economy of brain network organization[J]. Nat Rev Neurosci, 2012, 13(5): 336-349.

[36] Sporns O. Network attributes for segregation and integration in the human brain[J]. Curr Opin Neurobiol, 2013, 23(2): 162-171.

[37] Parlatini V, Radua J, Dell'acqua F, Leslie A, Simmons A, Murphy DG, Catani M, Thiebaut De Schotten M. Functional segregation and integration within fronto-parietal networks[J]. Neuroimage, 2017, 146(367-375.

[38] Lawrence AJ, Chung AW, Morris RG, Markus HS, Barrick TR. Structural network efficiency is associated with cognitive impairment in small-vessel disease[J]. Neurology, 2014, 83(4): 304-311.

[39] Zhang J, Wang J, Wu Q, Kuang W, Huang X, He Y, Gong Q. Disrupted brain connectivity networks in drug-naive, first-episode major depressive disorder[J]. Biol Psychiatry, 2011, 70(4): 334-342.

[40] Buhle J, Wager TD. Performance-dependent inhibition of pain by an executive working memory task[J]. Pain, 2010, 149(1): 19-26.

[41] Kong J, Jensen K, Loiotile R, Cheetham A, Wey HY, Tan Y, Rosen B, Smoller JW, Kaptchuk TJ, Gollub RL. Functional connectivity of the frontoparietal network predicts cognitive modulation of pain[J]. Pain, 2013, 154(3): 459-467.

[42] Riegel B, Bruenahl CA, Ahyai S, Bingel U, Fisch M, Löwe B. Assessing psychological factors, social aspects and psychiatric co-morbidity associated with Chronic Prostatitis/Chronic Pelvic Pain Syndrome (CP/CPPS) in men—a systematic review[J]. Journal of psychosomatic research, 2014, 77(5): 333-350.

[43] Ku JH, Kim SW, Paick J-S. Quality of life and psychological factors in chronic prostatitis/chronic pelvic pain syndrome[J]. Urology, 2005, 66(4): 693-701.

[44] Kutch JJ, Ichesco E, Hampson JP, Labus JS, Farmer MA, Martucci KT, Ness TJ, Deutsch G, Apkarian AV, Mackey SC. Brain signature and functional impact of centralized pain: a multidisciplinary approach to the study of chronic pelvic pain (MAPP) network study[J]. Pain, 2017, 158(10): 1979-1991.

[45] Shackman AJ, Salomons TV, Slagter HA, Fox AS, Winter JJ, Davidson RJ. The integration of negative affect, pain and cognitive control in the cingulate cortex[J]. Nature Reviews Neuroscience, 2011, 12(3): 154.

[46] Nevian T. The cingulate cortex: divided in pain[J]. Nature neuroscience, 2017, 20(11): 1515.

Figures

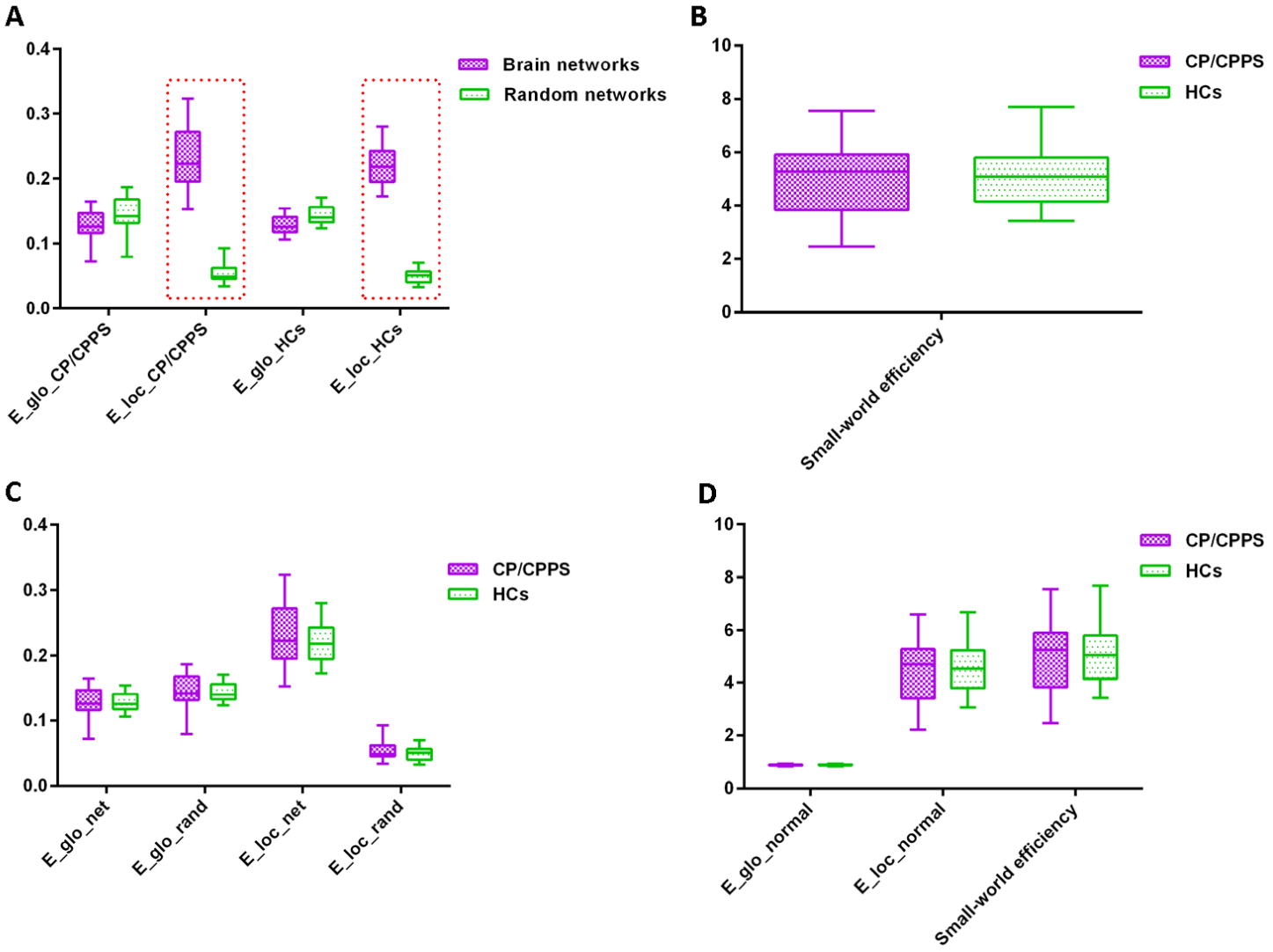

Figure 1

Topological organization of the whole WM brain network in CP/CPPS CP/CPPS: chronic prostatitis/chronic pelvic pain syndrome; HCs: health controls; WM: white matter. A and B: the small-world efficiency of the brain networks in CP/CPPS; C and D: the network efficiency of the whole brain in CP/CPPS. E_glo_net: the global efficiency of the brain network; E_glo_ rand: the global efficiency of the matched random networks; E_glo_ normal: the normalized global efficiency of the brain network; E_loc_net: the local efficiency of the brain network; E_loc_ rand: the local efficiency of the matched random networks; E_loc_ normal: the normalized local efficiency of the brain network. P<0.05 indicated significant between-groups differences. Red dotted box indicated that the brain networks of both CP/CPPS and HCs had a much higher local efficiency compared the matched random networks

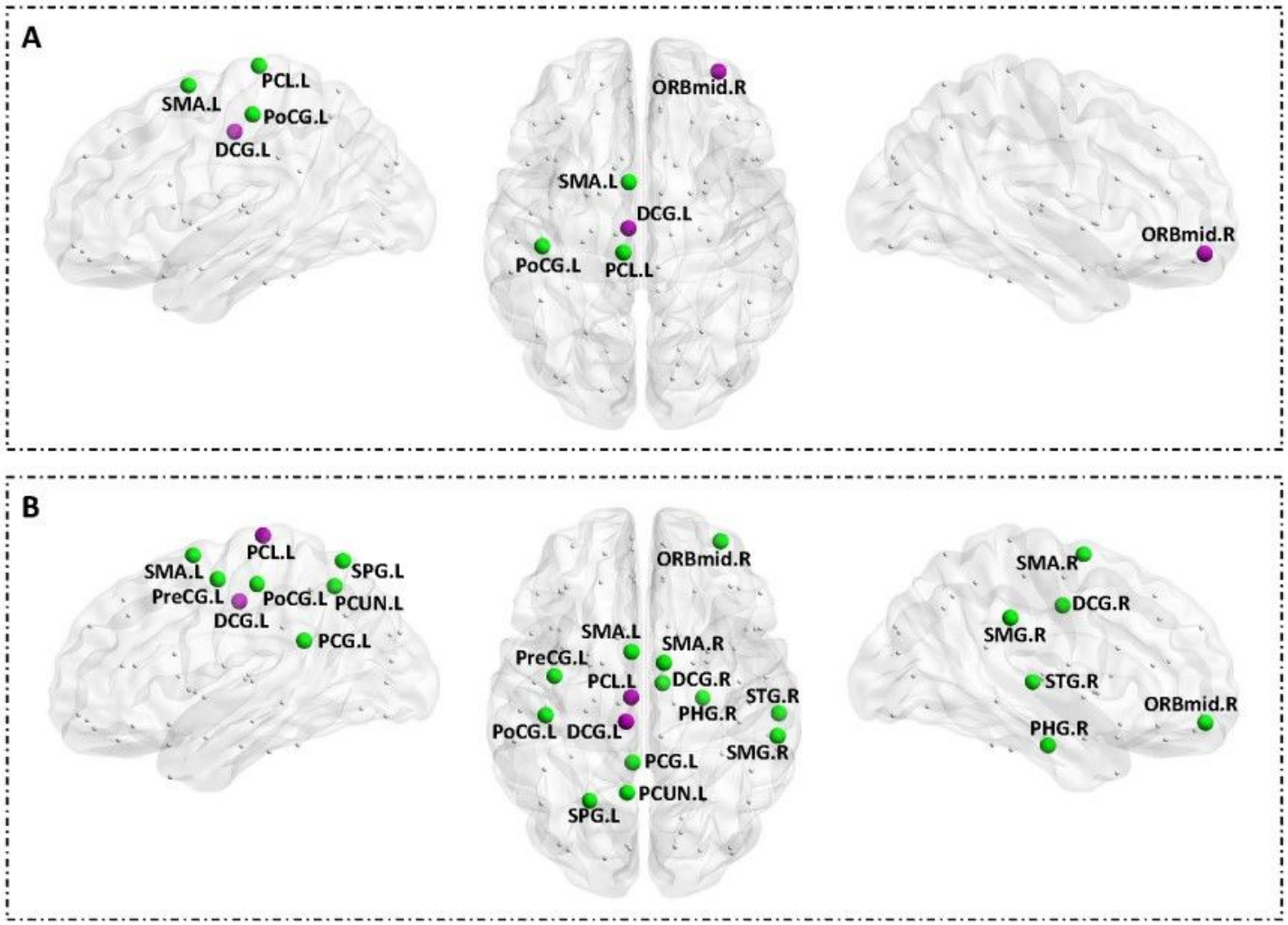

Figure 2

Regional nodal efficiency of the WM brain networks in CP/CPPS A: brain regions with abnormal global efficiency in CP/CPPS; B: brain regions with abnormal local efficiency in CP/CPPS. L: left; R: right; ORBmid: middle frontal gyrus (orbital part); SMA: supplementary motor area; DCG: middle cingulate and paracingulate gyri; PoCG: postcentral gyrus; PCL: paracentral lobule; PreCG: precental gyrus; SMA: supplementary motor area; PCG: posterior cingulate gyrus; PHG: parahippocampal gyrus; SPG: superior parietal gyrus; SMG: supramarginal gyrus; PCUN: precuneus; STG: superior temporal gyrus. P<0.05 indicated significant between-groups differences. Violet dots indicated the between-group differences survived FDR-correction; green dots indicated the between-group differences did not survive FDR-correction; gray dots indicated no between-group differences.

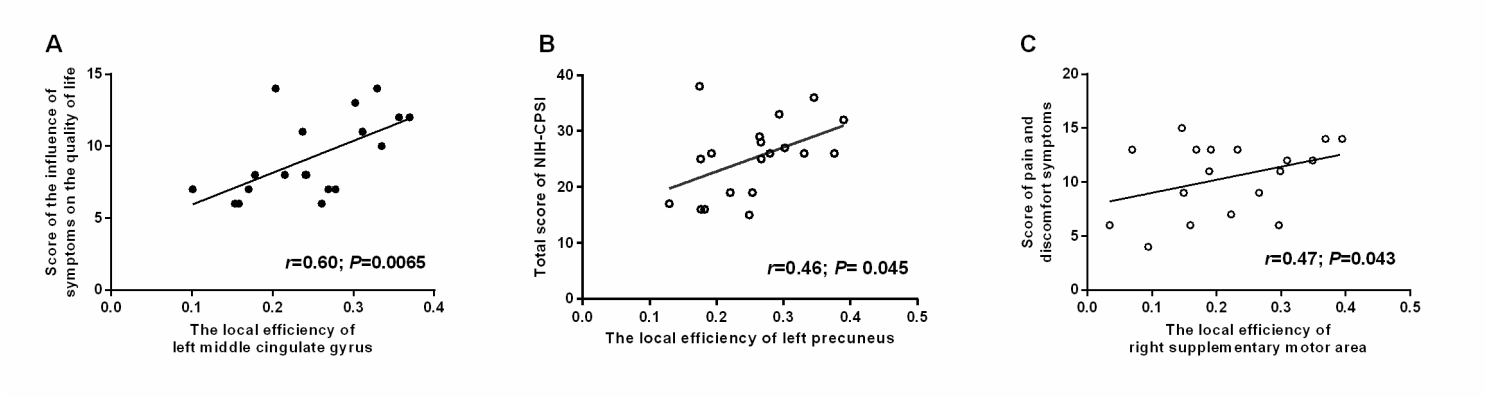

Figure 3

Relationships between altered nodal efficiency and NIH-CPSI Solid scatter indicated the correlation analysis of the altered brain regions that survived FDR-correction; hollow scatter indicated the correlation analysis of the altered brain regions that did not survive FDR-correction. P<0.05 indicated significant between-groups differences.